White Rose Research Online

eprints@whiterose.ac.uk
https://eprints.whiterose.ac.uk
Universities of Leeds, Sheffield and York

Deposited via The University of York.

White Rose Research Online URL for this paper:
https://eprints.whiterose.ac.uk/id/eprint/209258/

Version: Accepted Version

Article:
Yamada, Atsuya, Yamada, Michihiro, Kusumoto, Shuhei et al. (2024) Growth of all-epitaxial Co2MnSi/Ge/Co2MnSi vertical spin-valve structures on Si. Materials Science in Semiconductor Processing. 108140. ISSN: 1369-8001

https://doi.org/10.1016/j.mssp.2024.108140

Reuse
This article is distributed under the terms of the Creative Commons Attribution (CC BY) licence. This licence allows you to distribute, remix, tweak, and build upon the work, even commercially, as long as you credit the authors for the original work. More information and the full terms of the licence here:
https://creativecommons.org/licenses/

Takedown
If you consider content in White Rose Research Online to be in breach of UK law, please notify us by emailing eprints@whiterose.ac.uk including the URL of the record and the reason for the withdrawal request.

UNIVERSITY OF LEEDS University of Sheffield UNIVERSITY of York

Growth of all-epitaxial $Co_2MnSi/Ge/Co_2MnSi$ vertical spin-valve structures on Si

Atsuya Yamada[a], Michihiro Yamada[b,c,d], Shuhei Kusumoto[a], Julio A. do Nascimento[e,f], Connor Murrill[e,f], Shinya Yamada[b,a,d], Kentarou Sawano[g], Vlado K. Lazarov[e,f], Kohei Hamaya[b,a,d,*]

[a]*Department of Systems Innovation, Graduate School of Engineering Science, Osaka University, Toyonaka, Osaka 560-8531, Japan*
[b]*Center for Spintronics Research Network, Graduate School of Engineering Science, Osaka University, Toyonaka, Osaka 560-8531, Japan*
[c]*PRESTO, Japan Science and Technology Agency, Kawaguchi, Saitama 332-0012, Japan*
[d]*Spintronics Research Network Division, Institute for Open and Transdisciplinary Research Initiatives, Osaka University, Suita, Osaka 565-0871, Japan*
[e]*School of Physics, Engineering and Technology, University of York, Heslington, York YO10 5DD, United Kingdom*
[f]*York JEOL Nanocentre, Helix House, Science Park, University of York, Heslington, York YO10 5BR, United Kingdom*
[g]*Advanced Research Laboratories, Tokyo City University, Setagaya, Tokyo 158-0082, Japan*

Abstract

We explore epitaxial growth of $Co_2MnSi/Ge/Co_2MnSi$ vertical spin-valve structures on Si, where the Co_2MnSi (CMS) is expected to be a half-metallic material for spintronics. By combining solid phase epitaxy, low-temperature molecular beam epitaxy, and atomic layer termination techniques, we can grow an epitaxial Ge layer on CMS at 250 °C, where the atomic interdiffusion between Ge and CMS is suppressed. After further optimization of the growth condition of the Ge intermediate layer, all-epitaxial CMS/Ge/CMS vertically stacked structures with spin-valve like magnetization reversal processes are demonstrated. This vertically stacked structures can be utilized for vertical spin-valve devices with a Ge channel on Si.

Keywords: Ge, Co_2MnSi, spintronics, vertical spin-valve device

*Corresponding author: hamaya.kohei.es@osaka-u.ac.jp, Phone:+81-6-6850-6330, FAX:+81-6-6850-6330

1. Introduction

To date, semiconductor-based spintronic theories and technologies have been reported for spin-based light emitting diodes (LEDs) and field-effect transistors (FETs) [1–13]. In particular, some technologies for room-temperature electrical spin injection/detection in semiconductors have been developed in lateral spin-valve (LSV) devices [14–17]. The spin injection/detection efficiency at room temperature is still lower than 20% although the use of Co-based Heusler alloys, expected to be half-metallic materials, has been proposed for the spin injector and detector contacts in the LSV device structures [13, 17].

To improve the performance of spintronics devices with three-dimensional integration in semiconductors, we have further explored vertically stacked ferromagnet (FM)/germanium (Ge)/FM structures formed by molecular beam epitaxy (MBE) techniques [18–24], where Ge has higher electron and hole mobility than Si. Thus, Ge-based technologies are promising for next-generation CMOS transistors [25] and the high-quality growth of Ge layers on Si is further opening a way for achieving photonics on Si [26]. Thus far, we have fabricated all epitaxial vertically stacked FM/Ge/FM structures with top CoFe and bottom Fe_3Si electrodes on Si substrate [20] and observed spin-dependent transport properties at room temperature through a Ge intermediate layer in the vertical spin-valve (VSV) devices [21]. In addition, we experimentally estimated the very short room-temperature spin diffusion length (∼8.4 nm) of an undoped p-Ge intermediate layer on Fe_3Si from the thickness dependence of Ge layers on spin signals [23]. Recently, we enhanced magnetoresistance (MR) effect at room temperature in all-epitaxial VSV devices with a Ge intermediate layer and a bottom Co_2FeSi (CFS) [24], in which CFS is one of the Co-based Heusler alloys with high spin polarization [27]. Unfortunately, we found that the chemical reaction and interdiffusion between Ge and CFS occurred, giving rise to the degradation of the spin injection/detection efficiency at room temperature [28].

Here we focus on another Co-based Heusler alloy, Co_2MnSi (CMS), instead of CFS. CMS is well known as a highly spin polarized material [29] and can be utilized for magnetic tunnel junctions [30–32], CPP-GMR [33], semiconductor-based LSV devices [34], and oxide-based structures [35, 36]. While, in general, it was very difficult to grow an epitaxial CMS on group-IV semiconductors [37–39], we grew an epitaxial CMS layer on Ge (111) without reaction layer owing to Fe atomic layer insertion by low-temperature

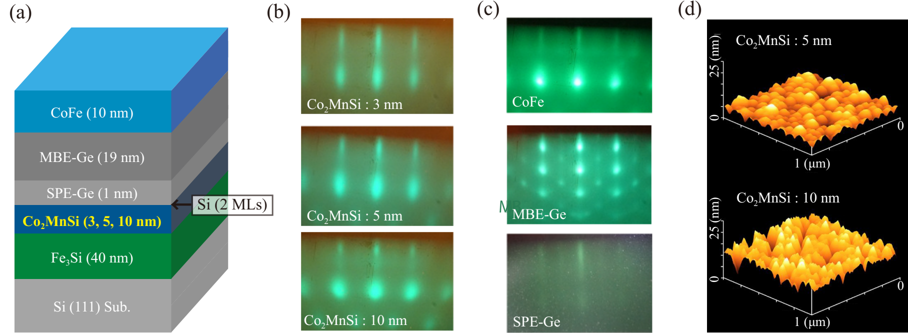

Figure 1: (a) Schematic of the grown CoFe/Ge/Co_2MnSi structure on Fe_3Si/Si(111). (b) RHEED images of the surface for a Co_2MnSi layer on Fe_3Si/Si(111) when the thickness of Co_2MnSi is 3, 5, and 10 nm. (c) RHEED images of the surface for CoFe, MBE-Ge, and SPE-Ge layers during the growth when the thickness of Co_2MnSi is 5 nm. (d) AFM images of the surface for the grown CoFe/Ge/Co_2MnSi structure when the thickness of Co_2MnSi is 5 and 10 nm.

MBE techniques in our recent work [40]. Moreover, for Ge-based LSV devices with a CMS/Ge heterostructure, we observed the large MR effect at room temperature [40]. Therefore, the growth of VSV structures with a CMS/Ge structure should be explored for high-performance semiconductor spintronic devices.

In this study, we experimentally demonstrate the growth of CMS/Ge/CMS vertical structures on Si for VSV devices. In particular, we explore the epitaxial growth with combining solid phase epitaxy (SPE), low-temperature MBE and atomic layer termination techniques. The detailed growth conditions, structural, and magnetic properties are discussed. This work paves the way for high-performance semiconductor-based VSV applications on Si.

2. Growth of a vertically stacked CoFe/Ge/Co_2MnSi on Si(111)

In this section, we explore the growth of epitaxial Ge layers on CMS. Here we utilized an established vertical structure consisting of CoFe, Ge, and Heusler alloy, on Si(111), as illustrated in Fig. 1(a) [20, 21, 24]. In the following, we explain the growth procedure and configuration of a CoFe/Ge/CMS VSV structure on Si(111). First, a 40 nm-thick Fe_3Si layer was grown as a buffer layer on Si(111) below 80 °C by low-temperature MBE [41, 42] because it is very difficult to grow an epitaxial CMS on group-IV semiconductors

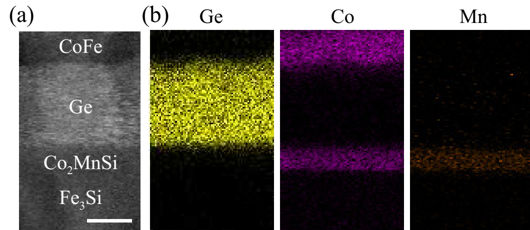

Figure 2: (a) Bright-field-STEM image of CoFe/Ge/Co_2MnSi/Fe_3Si structure on Si(111) substrate. (b) EDX mapping images for Ge, Co, and Mn from the same region shown in (a). Scale bar in (a) is 10 nm.

[39]. Next, we grew a CMS layer below 80 °C with different thicknesses of 3, 5, and 10 nm on the Fe_3Si buffer layer [40]. As shown in *in-situ* reflection high energy electron diffraction (RHEED) images of Fig. 1(b), two-dimensional epitaxial growth of the CMS layers is seen. However, with increasing the thickness of the CMS layer, the RHEED patterns gradually change from streak to spotty. After confirming the epitaxial growth, the surface of the CMS layer was continuously terminated with two monolayers (MLs) of Si for the epitaxial growth of the Ge layer on top of it [18].

On top of the Si-terminated CMS, we also grew a 20 nm-thick Ge layer by SPE and MBE to obtain the smooth surface [20]: A 1 nm-thick amorphous Ge layer was deposited at room temperature, and then, the substrate temperature was raised up to 250°C for crystallization of Ge. A weak streak pattern of the RHEED image of the surface for the SPE-Ge layer is still visible in the bottom of Fig. 1(c) (Here, the CMS thickness is 5 nm). Subsequently, we grew a 19 nm-thick Ge layer by MBE at the same temperature as SPE-crystallization temperature. As seen in the center of Fig. 1(c), the RHEED image of the surface for the MBE-Ge layer includes spotty patterns. Finally, we grew a 10 nm-thick CoFe layer on the MBE-Ge layer. We can also see the spotty patterns of the CoFe layer, superimposed on the streak patterns in the top of Fig. 1(c). As a result, an all-epitaxial CoFe/Ge/Co_2MnSi structure on Fe_3Si/Si(111) was obtained. After the growth, we evaluate the flatness for the grown CoFe/Ge/CMS VSV structures by atomic force microscopy (AFM), as shown in Fig. 1(d). When the thickness of the CMS layer is 5 nm, we obtain a sufficient flatness for spintronic devices, in which root-mean-square roughness (R_{rms}) is ∼1.1 nm. On the other hand, when that is 10 nm, the value of

R_{rms} becomes $\sim$2.3 nm, about twice as large as that for the 5-nm-thick CMS. Since the 3-nm-thick CMS layer may be too thin to observe the highly efficient spin injection in VSV devices, we conclude that the 5 nm-thick CMS layer is available for the bottom CMS electrodes in the VSV device on Si.

3. Evaluation of the grown CoFe/Ge/Co_2MnSi structure

We carried out further structural investigations by cross-sectional scanning transmission electron microscopy (STEM) and energy dispersive x-ray spectroscopy (EDX) measurements. Figure 2 shows a cross-sectional bright-field-STEM image [(a)] and EDX elemental mappings [(b)] for the vertically stacked CoFe/Ge/CMS(5 nm)/Fe_3Si structure. From the EDX elemental mappings, it can be seen that the CoFe, Ge, and CMS layers are clearly separated, and Co and Mn atoms are detected in the range of $\sim$5 nm below the Ge intermediate layer. It is indicated that the atomic interdiffusion between Ge and CMS is nearly suppressed at the interface. This feature is markedly different from the Ge/CFS interface reported in previous work [28].

Next, we measured the magnetic properties by vibrating sample magnetometer (VSM). Figure 3 shows a magnetic field (H) dependence of magnetization (M) (M-H curve) at room temperature for the CoFe/Ge/CMS(5 nm) structure on Fe_3Si/Si(111). We observe a difference in the two magnetization states between the top CoFe and the bottom CMS/Fe_3Si layers. Also, the value of the saturation magnetization for this structure is nearly consistent with the theoretical value of $\sim$910 emu/cm^3 [20, 29, 43]. This means that the top and bottom layers are magnetically decoupled via the Ge layer and the chemical reaction between the Ge and CMS layers are almost suppressed because of the low-temperature growth of Ge with combining SPE and MBE at 250°C. Therefore, we conclude that an all-epitaxial CoFe/Ge/CMS vertical structure with spin-valve-like magnetization reversal processes is successfully obtained on Si(111).

4. Demonstration of all-epitaxial Co_2MnSi/Ge/Co_2MnSi structures on Si

We finally try to grow a top CMS layer on the Ge intermediate layer for an all-epitaxial CMS/Ge/CMS VSV structure. To further improve the quality of the CMS

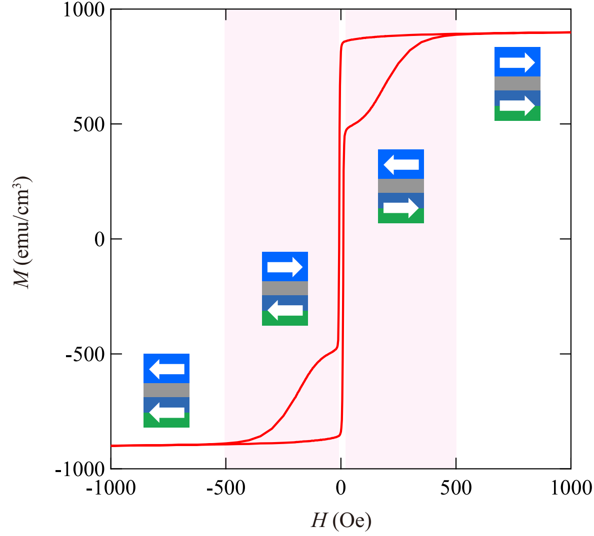

Figure 3: Room-temperature M-H curve of an all-epitaxial CoFe/Ge/Co_2MnSi/Fe_3Si structure. The insets mean the magnetization states between the top CoFe and bottom Co_2MnSi/Fe_3Si layers. The pink region means antiparallel magnetization state.

layer, we utilize a Germanium-on-Silicon (GOS) substrate consisting of a 240-nm-thick Ge buffer layer and Si(111) utilizing a two-step growth technique by MBE [44], as shown in Fig. 4(a). Here the lattice mismatch between Fe_3Si and Ge is almost zero [45]. Next, a 40 nm-thick Fe_3Si layer and a 5-nm-thick CMS layer was grown on the GOS substrate below 80 °C by low-temperature MBE and the surface was terminated with two monolayers of Si as mentioned before [18]. On top of the Si-terminated CMS, we explored the growth condition of the Ge intermediate layer by combining SPE and MBE because a top CMS layer became a polycrystalline film even in the same condition for the top CoFe layer, described in previous section.

To demonstrate epitaxial growth of the top CMS layer, we also try to improve the crystallinity of the Ge intermediate layer. As a result, when we changed the thickness of SPE-grown Ge from 1 nm to 2 nm at 250°C, the RHEED image of the surface of the SPE-Ge layer became clear [Fig. 4(b)], leading to the epitaxial Ge layer with high crystallinity. After the growth of 28 nm-thick Ge by MBE at the same temperature (250°C), we can clearly see streak patterns of the surface of the MBE-grown Ge [Fig.

4(b)], different from the spotty patterns shown in the center of Fig. 1(c). Furthermore, to induce the crystallization of a top CMS layer, the surface of the MBE-grown Ge layer is terminated with 5 MLs of Fe [40]. Here the terminated Fe layer also plays an important role for an enhancement in the spin injection/detection efficiency at the Co-based Heusler/Ge interfaces at room temperature [46, 47]. On top of the Fe-terminated Ge layer, a 3-nm-thick CMS layer as a top FM electrode is grown below 80 °C [40]. As a consequence, the RHEED image of the top CMS layer shows a streak pattern, indicating the two-dimensional epitaxial growth of the CMS layer. Even on the Ge intermediate layer, we demonstrate the epitaxial CMS layer for the first time, meaning that an all-epitaxial CMS/Ge/CMS structure is grown on Si. Finally, we grew a 7-nm-thick CoFe layer to make the difference in the magnetization switching fields between the top and bottom CMS layers.

Figure 4(c) shows an M-H curve measured by VSM at room temperature for the all-epitaxial CoFe/CMS/ Ge/CMS/Fe_3Si structure on the GOS substrate. Clear spin-valve like magnetization reversal processes are observed at room temperature, meaning that the top CoFe/CMS and the bottom CMS/Fe_3Si layers are magnetically decoupled via the Ge intermediate layer. Also, the value of the saturation magnetization is nearly consistent with the theoretical value ($\sim$ 880 emu/cm^3) [20, 29, 43].

Finally, we conduct the detailed structural analyses for the CoFe/CMS/Ge/CMS/Fe_3Si structure in Fig. 5. From the EDX elemental mappings, it can be seen that the CoFe, top CMS, Ge, and bottom CMS layers are clearly separated, and Co, Mn and Si atoms are detected in the range of $\sim$3 nm above the Ge intermediate layer as well as the range of $\sim$5 nm below the Ge intermediate layer. The Fe atomic termination layer between top CMS and Ge layers is distinctively observed. It is indicated that the atomic interdiffusion between the top CMS, the Ge intermediate and the bottom CMS layers is nearly suppressed at the interface by combining SPE, low-temperature MBE, and the Fe atomic layer termination technique [20, 40, 46]. From these results, we conclude that an all epitaxial CMS/Ge/CMS VSV structure is successfully demonstrated on a Si platform. This structure paves the way for high-performance semiconductor-based VSV applications on Si.

5. Conclusion

We explored epitaxial growth of Co_2MnSi/Ge/Co_2MnSi vertical spin-valve structures on Si. By combining SPE, low-temperature MBE, and atomic layer termination techniques, we grew an epitaxial Ge layer on CMS at 250 °C, where the atomic interdiffusion between Ge and CMS was suppressed. After further optimization of the growth condition of the Ge intermediate layer, all-epitaxial CMS/Ge/CMS vertically stacked structures with spin-valve like magnetization reversal processes were demonstrated. This vertical structures can be utilized for vertical spin-valve devices with a Ge channel on Si.

Acknowledgment

We acknowledge Prof. Y. Suzuki and Prof. Y. Niimi for lots of experimental supports. This work was supported by JST PRESTO (No. JPMJPR20BA), JSPS KAKENHI (Grants No. 19H05616 and 21H05000), JST CREST (Grant No. JPMJCR23A5), the Spintronics Research Network of Japan (Spin-RNJ), and MEXT, X-NICS (Grant No. JPJ011438). A. Yamada acknowledges JSPS Research Fellowship for Young Scientists (Grant No. 23KJ1446) and the Program for Leading Graduate Schools: "Interactive Materials Science Cadet Program".

References

[1] S. Datta and B. Das, Appl. Phys. Lett. 56 (1990) 665.

[2] Y. Ohno, D. K. Young, B. Beschoten, F. Matsukura, H. Ohno, and D. D. Awschalom, Nature (London) 402 (1999) 790.

[3] A. Fert and H. Jaffrès, Phys. Rev. B 64 (2001) 184420.

[4] A. T. Hanbicki, B. T. Jonker, G. Itskos, G. Kioseoglou, and A. Petrou, Appl. Phys. Lett. 80 (2002) 1240.

[5] I. Žutić, J. Fabian and S. D. Sarma, Rev. Mod. Phys. 76 (2004) 323.

[6] A. M. Bratkovsky, Rep. Prog. Phys. 71 (2008) 026502.

[7] H. Dery, P. Dalal, Ł. Cywiński, and L. J. Sham, Nature 447 (2007) 573-576.

[8] M. Tanaka and S. Sugahara, IEEE Trans. Electron Devices 54 (2007) 961.

[9] X. Lou, C. Adelmann, S. A. Crooker, E. S. Garlid, J. Zhang, K. S. M. Reddy, S. D. Flexner, C. J. Palmstrøm, and P. A. Crowell, Nat. Phys. 3 (2007) 197.

[10] P. Bruski, Y. Manzke, R. Farshchi, O. Brandt, J. Herfort, and M. Ramsteiner, Appl. Phys. Lett. 103 (2013) 052406.

[11] I. Appelbaum, B. Huang, and D. J. Monsma, Nature (London) 447 (2007) 295.

[12] K. Hamaya, Y. Fujita, M. Yamada, M. Kawano, S. Yamada, and K. Sawano, J. Phys. D: Appl. Phys. 51 (2018) 393001.

[13] K. Hamaya and M. Yamada, MRS Bull. 47 (2022) 584.

[14] T. Suzuki, T. Sasaki, T. Oikawa, M. Shiraishi, Y. Suzuki, and K. Noguchi, Appl. Phys. Express 4 (2011) 023003.

[15] M. Yamada, M. Tsukahara, Y. Fujita, T. Naito, S. Yamada, K. Sawano, and K. Hamaya, Appl. Phys. Express 10 (2017) 093001.

[16] S. Yamada, M. Kato, S. Ichikawa, M. Yamada, T. Naito, Y. Fujiwara, and K. Hamaya, Adv. Electron. Mater. 9 (2023) 2300045.

[17] T. Naito, M. Yamada, Y. Wagatsuma, K. Sawano, and K. Hamaya, Phys. Rev. Applied 18 (2022) 024005.

[18] S. Yamada, K. Tanikawa, M. Miyao, and K. Hamaya, Cryst. Growth Des. 12 (2012) 4703.

[19] M. Kawano, M. Ikawa, K. Arima, S. Yamada, T. Kanashima, and K. Hamaya, J. Appl. Phys. 119 (2016) 045302.

[20] S. Sakai, M. Kawano, M. Ikawa, H. Sato, S. Yamada, and K. Hamaya, Semicond. Sci. Technol. 32 (2017) 094005.

[21] M. Kawano, M. Ikawa, K. Santo, S. Sakai, H. Sato, S. Yamada, and K. Hamaya, Phys. Rev. Mater. 1 (2017) 034604.

[22] T. Shiihara, M. Yamada, M. Honda, A. Yamada, S. Yamada, and K. Hamaya, Appl. Phys. Express 13 (2020) 023001.

[23] A. Yamada, M. Yamada, T. Shiihara, M. Ikawa, S. Yamada, and K. Hamaya, J. Appl. Phys. 129 (2021) 013901.

[24] A. Yamada, M. Yamada, M. Honda, S. Yamada, K. Sawano, and K. Hamaya, Appl. Phys. Lett. 119 (2021) 192404.

[25] A. Toriumi and T. Nishimura, Jpn. J. Appl. Phys. 57 (2018) 010101.

[26] Y. Kang, H.-D. Liu, M. Morse, M. J. Paniccia, M. Zadka, S. Litski, G. Sarid, A. Pauchard, Y.-H. Kuo, H.-W. Chen, W. S. Zaoui, J. E. Bowers, A. Beling, D. C. McIntosh, X. Zheng, and J. C. Campbell, Nature Photonics 3 (2009) 59-63.

[27] K. Hamaya, N. Hashimoto, S. Oki, S. Yamada, M. Miyao, and T. Kimura, Phys. Rev. B 85 (2012) 100404(R).

[28] M. Yamada, S. Kusumoto, A. Yamada, K. Sawano, and K. Hamaya, Mater. Sci. Semicond. Proc. 171 (2024) 107987.

[29] B. Balke, G. H. Fecher, H. C. Kandpal, C. Felser, K. Kobayashi, E. Ikenaga, J.-J. Kim, and S. Ueda, Phys. Rev. B 74 (2006) 104405.

[30] Y. Sakuraba, M. Hattori, M. Oogane, Y. Ando, H. Kato, A. Sakuma, and T. Miyazaki, Appl. Phys. Lett. 88 (2006) 192508.

[31] M. Yamamoto, T. Ishikawa, T. Taira, G.f. Li, K. Matsuda, and T. Uemura, J. Phys.: Condens. Matter 22 (2010) 164212.

[32] R. Fetzer, S. Ouardi, Y. Honda, H. Liu, S. Chadov, B. Balke, S. Ueda, M. Suzuki, T. Uemura, M. Yamamoto, M. Aeschlimann, M. Cinchetti, G. H. Fecher, and C. Felser, J. Phys. D 48 (2015) 164002.

[33] K. Yakushiji, K. Saito, S. Mitani, K. Takanashi, Y.K. Takahashi, and K. Hono, Appl. Phys. Lett. 88 (2006) 222504.

[34] Z. Lin, D. Pan, M. Rasly, and T. Uemura, Appl. Phys. Lett. 114 (2019) 012405.

[35] K. Kudo, Y. Hamazaki, S. Yamada, S. Abo, Y. Goda, and K. Hamaya, ACS Appl. Electron. Mater. 1 (2019) 2371-2379.

[36] K. Kudo, S. Yamada, M. Yafuso, T. Kimura, V. K. Lazarov, and K. Hamaya, J. Alloys Compd. 854 (2021) 155571.

[37] M. A. I. Nahid, M. Oogane, H. Naganuma, and Y. Ando, Appl. Phys. Lett. 96 (2010) 142501.

[38] S. Yamada, K. Hamaya, T. Murakami, B. Varaprasad, Y. K. Takahashi, A. Rajanikanth, K. Hono, and M. Miyao, J. Appl. Phys. 109 (2011) 07B113.

[39] M. Kawano, S. Yamada, S. Oki, K. Tanikawa, M. Miyao, and K. Hamaya, Jpn. J. Appl. Phys. 52 (2013) 04CM06.

[40] K. Kudo, M. Yamada, S. Honda, Y. Wagatsuma, S. Yamada, K. Sawano, and K. Hamaya, Appl. Phys. Lett. 118 (2021) 162404.

[41] K. Hamaya, K. Ueda, Y. Kishi, Y. Ando, T. Sadoh, and M. Miyao, Appl. Phys. Lett. 93 (2008) 132117.

[42] S. Oki, S. Yamada, K. Tanikawa, K. Yamasaki, M. Miyao, and K. Hamaya, Appl. Phys. Lett. 103 (2013) 212402.

[43] M. Ikawa, M. Kawano, S. Sakai, S. Yamada, T. Kanashima, and K. Hamaya, Journal of Crystal Growth 468 (2017) 676-679.

[44] K. Sawano, Y. Hoshi, S. Kubo, K. Arimoto, J. Yamanaka, K. Nakagawa, K. Hamaya, M. Miyao, and Y. Shiraki, Thin Solid Films 613 (2016) 24.

[45] S. Yamada, J. Sagar, S. Honda, L. Lari, G. Takemoto, H. Itoh, A. Hirohata, K. Mibu, M. Miyao, and K. Hamaya, Phys. Rev. B 86 (2012) 174406.

[46] M. Yamada, F. Kuroda, M. Tsukahara, S. Yamada, T. Fukushima, K. Sawano, T. Oguchi, and K. Hamaya, NPG Asia Mater. 12 (2020) 47.

[47] M. Yamada, Y. Shiratsuchi, H. Kambe, K. Kudo, S. Yamada, K. Sawano, R. Nakatani, and K. Hamaya, J. Appl. Phys. 129 (2021) 183901.

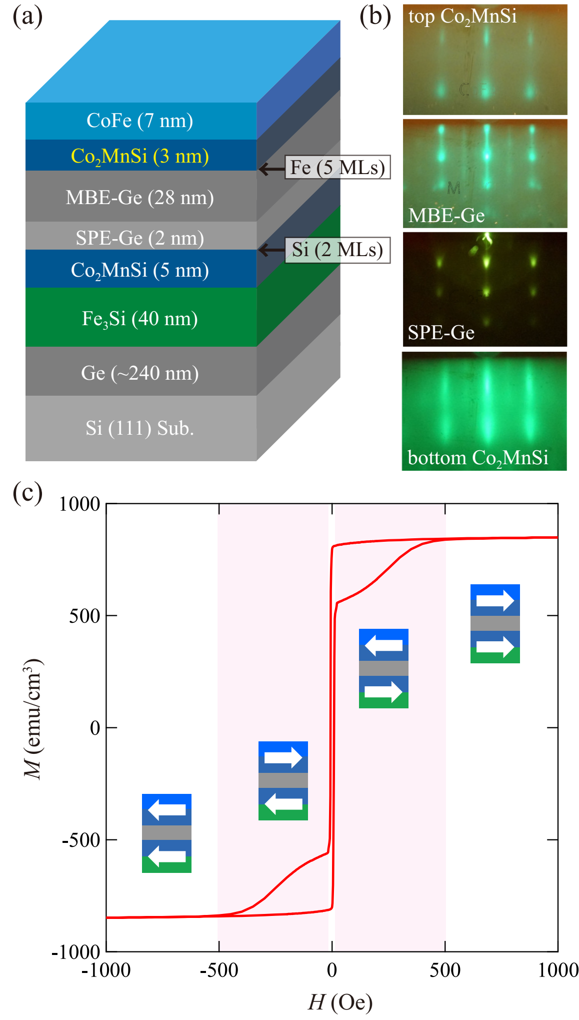

Figure 4: (a) Schematic of the grown CoFe/Co_2MnSi/Ge/Co_2MnSi structure on Fe_3Si/GOS(111). (b) RHEED images of the surface for top Co_2MnSi, MBE-Ge, SPE-Ge and bottom Co_2MnSi layers during the growth. (c) Room-temperature M-H curve of the structure. The insets mean the magnetization states between the top CoFe/Co_2MnSi and bottom Co_2MnSi/Fe_3Si layers. The pink region means the antiparallel magnetization state.

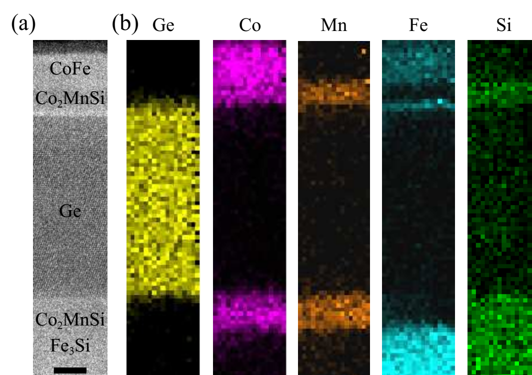

Figure 5: (a) High-angle annular dark-field STEM image of a $CoFe/Co_2MnSi/Ge/Co_2MnSi/Fe_3Si$ structure on GOS(111). (b) EDX mapping images for Ge, Co, Mn, Fe and Si from the same region shown in (a). Scale bar in (a) is 5 nm.